

---

## Study on Air Pollution and Its Dispersion Pattern in Pokhara Valley

Rajib Pokhrel<sup>1\*</sup>

*School of Engineering, Faculty of Science and Technology, Pokhara University, Nepal*

Corresponding email: [rajibp@pu.edu.np](mailto:rajibp@pu.edu.np)



Pokhara Engineering College Journal (ISSN: 3021-9795), Copyright © [2025] The Author(s). Published by Pokhara Engineering College, distributed under the terms of the Creative Commons Attribution 4.0 International License (CC BY-NC 4.0).

*Received: 29-December-2024; Revised: 26-January-2025; Accepted: 30-January-2025*

---

### Abstract

Regional International Airport has been in operation in the mid of Pokhara Metropolitan City where most of the farming land has been converted to the built-up area. Distinct temperature difference has been felt in between downtown and nearby sub-urban area. This study was conducted to investigate the wind flow pattern and air pollution dispersion mechanism in Pokhara. A numerical simulation technique such as A2C flow / A2C t & d was introduced to simulate the local wind flow vectors and air pollution (puffs) dispersion by locally generated

wind in the study domain. The simulation results for the study domain revealed that the air flows from the mountain region to the valley from the mid-night to the early morning around 8 AM. As the mountain region get heated after the sunshine, the flow velocity decreases and reaches to the transition state around 09:00 – 10:00 AM. Then flow direction changes towards the mountain region after 11 AM and the velocity reaches the maximum around 2 PM to 3 PM. It is continuous till mid-night around 9 PM to 10 PM and again reaches to the transition period. The locally generated wind plays significant role for the transport and dispersion of air pollution (puff) generated from the source to the surrounding region. Generally, urban air pollution generated in the valley area accumulated in the valley region in the mid-night to the early morning and it disperses around the upper air mostly above the mountain region. Mostly, the pollution generated nearby the mountain region disperses above the mountain region in the daytime. Hence it is concluded that the pollution generated from the difference sources such as aviation, automobiles, industries and the construction sites in the periphery of Pokhara Metropolitan City disperses around the Valley and reached up to the nearby mountain region.

**Keywords:** *Air Pollution, Air Dispersion, Meteorology, Numerical Simulation*

---

### 1. Introduction

Construction activities, automobiles have been notably increasing in Pokhara with the increase of population. Its natural beauty has been deteriorating day by day due to the increased pollution as well as haphazard urbanization. Recently, numbers of road development, residential / commercial building construction activities, construction and operation of mega projects such as Pokhara International Airport, Prithvi Highway, number of industries, etc. have been in operation stage in Pokhara which noticeably impacted the air quality of the Valley. In general, construction practice in Nepal is open, while air emissions such as Particulate Matters (PM), gaseous emissions, etc. easily disperse in the atmospheric environment.



**Figure 1.** Major sources of air pollution in Pokhara; (a) Stack emission from the Industrial area and (b) dust dispersion in the construction site during the construction stage.

A mega project, new international airport was in construction phase since 13 April 2016 in the centre of Pokhara Metropolitan City and it has already been in operation where particulate emission deteriorates the visibility around the Pokhara as in Fig. 1(b). Earth moving operations is the most important contributor of PM emissions across the construction industry where truck loading and dumping of crushed rocks and mud, and dirt carryout from construction site to the destination via adjoining roads are major sources of PM emission. Moreover, most of the industries operated in Pokhara Industrial Estate emitted the air pollution as in Fig. 1(a) which may noticeably contributed the particulate as well as gaseous pollutant in the surrounding area.

There are three real time air quality monitoring station in Pokhara Valley at (a) Gandaki Boarding School, (b) DHM Pokhara and (c) Pokhara University. Some stations data have been updated at the website for public information but cannot download the detail data for research and analysis purpose. There was not a real time air quality monitoring system near the airport construction area therefore it is difficult to identify how much the air pollution was added from the airport construction activity in Pokhara valley and its effective zone around Pokhara. Moreover, approximately 200 ha of firm land has been converted to concrete and constructed land as Pokhara International Airport in the heart of Pokhara. In the recent decade, the land use pattern in the Pokhara Valley noticeably changed to the built-up area as an Airport, residential and commercial area which may affect the local meteorology and air dispersion mechanism too. Lana et al. reported that the stable meteorological condition overshadowed the air pollution level in the city (Laña et al., 2016). Wind influences the dispersion of air pollutants. Strong winds can dilute pollutant concentrations by dispersing them over a larger area, while stagnant conditions (low wind speed) can lead to the accumulation of pollutants. The direction of the wind also determines where pollutants are transported, potentially affecting regions far from their source (Jacob, 1999). In urban area, most of the land is covered with civil structures, consequently the urban areas experience unique meteorological conditions due to the urban heat island (UHI) effect, which exacerbates pollutant concentrations (Wond and Chen, 2009). Therefore, numerical simulation techniques such as Lagrangian approach (A2C model) has been introduced in this research to understand the air dispersion pattern and estimate air pollution dispersion zone in the Pokhara valley. A2C model has already been widely used for such study around the world as it is built up with effective numerical approach in simple operating procedure which takes less time and space for the simulation (Pokhrel and Lee, 2011; Pokhrel and Ghimire, 2020).

## 2. Air Dispersion Modelling

Modeling technique is an essential tool for atmospheric environmental studies together with observational data. Models are based upon semi-empirical statistical relations among available data and measurements. This study introduced the air dispersion in the study area using computer modelling based on the Lagrangian Approach. A2C (Atmospheric to Computational fluid dynamics) flow and A2C t&d (transport & diffusion) are the updated versions of HOTMAC and RAPTAD, respectively. The basic equations of HOTMAC for mean wind, temperature, mixing ratio of water vapour, and turbulence are similar to those used by Yamada (1981, 1985). It has the addition of nested grid capability and the effect of shadows produced by the terrain. The terrain vertical coordinate system is used in this model in order to increase the accuracy in the treatment of surface boundary conditions.

$$z^* = \bar{H} \frac{z - z_g}{H - z_g} \quad (1)$$

Where  $z^*$  and  $z$  are the transformed and Cartesian-vertical coordinates, respectively;  $z_g$  is ground elevation;  $\bar{H}$ , the material surface top of the model in the  $z^*$  coordinate; and  $H$ , the corresponding height in the  $z$  - coordinate. The governing equations following the coordinate transformation based on Yamada (1981) (Yamada, 1981) are

$$\frac{DU}{Dt} = f(V - V_g) + g \frac{\bar{H} - z^*}{\bar{H}} \left( 1 - \frac{\langle \theta_v \rangle}{\theta_v} \right) \frac{\partial z_g}{\partial x} + \frac{\partial}{\partial x} \left( K_x \frac{\partial U}{\partial x} \right) + \frac{\partial}{\partial y} \left( K_{xy} \frac{\partial U}{\partial y} \right) + \frac{\bar{H}}{H - z_g} \frac{\partial}{\partial z^*} (\overline{-uw}) \quad (2)$$

$$\frac{DV}{Dt} = -f(U - U_g) + g \frac{\bar{H} - z^*}{\bar{H}} \left( 1 - \frac{\langle \theta_v \rangle}{\theta_v} \right) \frac{\partial z_g}{\partial y} + \frac{\partial}{\partial x} \left( K_{xy} \frac{\partial V}{\partial x} \right) + \frac{\partial}{\partial y} \left( K_y \frac{\partial V}{\partial y} \right) + \frac{\bar{H}}{H - z_g} \frac{\partial}{\partial z^*} (\overline{-vw}) \quad (3)$$

$$\frac{\partial U}{\partial x} + \frac{\partial V}{\partial y} + \frac{\partial W^*}{\partial z^*} - \frac{1}{H - z_g} \left( U \frac{\partial z_g}{\partial x} + V \frac{\partial z_g}{\partial y} \right) = 0 \quad (4)$$

Where,

$$W^* = \frac{\bar{H}}{H - z_g} W + \frac{z^* - \bar{H}}{H - z_g} \left( U \frac{\partial z_g}{\partial x} + V \frac{\partial z_g}{\partial y} \right) \quad (5)$$

and

$$\frac{D(\cdot)}{Dt} = \frac{\partial(\cdot)}{\partial t} + U \frac{\partial(\cdot)}{\partial x} + V \frac{\partial(\cdot)}{\partial y} + W^* \frac{\partial(\cdot)}{\partial z^*} \quad (6)$$

In the above expression  $\langle \rangle$  indicates an average over a horizontal surface.  $\theta_v = ((P_0 / P)^{R/C_p} (1 + 0.61Q_v) T)$  is the virtual potential temperature;  $f$  for coriolis parameter;  $g$  for acceleration of gravity;  $P$  for pressure;  $P_0$  for a reference pressure;  $C_p$  for specific heat capacity of dry air at constant pressure ( $=1.003 \text{ Jg}^{-1} \text{ K}^{-1}$ );  $R$  for gas constant for dry air ( $=0.28704 \text{ Jg}^{-1} \text{ K}^{-1}$ );  $Q_v$  for mixing ratio of water vapor;  $U, V, W$  for mean velocity in  $x, y, z$  directions, respectively;  $u, v, w$  for velocity fluctuations. The second term on the right-hand side of eq. (2) and eq. (3) indicate the effect of ground slope. For simplicity,  $H$  is specified as

$$H = \bar{H} + z_{g \max} \quad (7)$$

Where,  $\bar{H} = 5000 \text{ m}$  as suggested by Yamada et al. (1999) (Yamada, 1999) and  $z_{g \max}$  is generated based on topographic data. Expressions of the horizontal eddy viscosity coefficients  $K_x$ ,  $K_y$ , and  $K_{xy}$ , are referred from Yamada (1978) (Yamada, Kao and Bunker, 1989). Similarly, the equations for the computation of geostrophic winds  $U_g$  and  $V_g$  are referred from Yamada (1981) (Yamada, 1981).

Concentration distributions are assumed in different forms and one of the simplest ways is to assume a Gaussian distribution where variances are determined as the time integration of the velocity variances encountered over the history of the puff. The concentration level at a given time and place is calculated as the sum of the concentrations from each puff (Yamada, 1999). Concentration  $C$  at  $(X, Y, Z)$  is computed by using the equation (11).

$$C(X, Y, Z) = \frac{Q\Delta t}{(2\pi)^{3/2}} \sum_{k=1}^N \frac{1}{\sigma_{xk} \sigma_{yk} \sigma_{zk}} \exp\left[-\frac{1}{2} \frac{(x_k - X)^2}{\sigma_{xk}^2}\right] \times \exp\left[-\frac{1}{2} \frac{(y_k - Y)^2}{\sigma_{yk}^2}\right] \\ \times \left\{ \exp\left[-\frac{1}{2} \frac{(y_k - Y)^2}{\sigma_{yk}^2}\right] + \exp\left[-\frac{1}{2} \frac{(z_k + Z - 2z_g)^2}{\sigma_{zk}^2}\right] \right\} \quad (8)$$

Where  $(x_k, y_k, z_k)$  is the location of the  $k^{\text{th}}$  puff;  $\sigma_{xk}$ ,  $\sigma_{yk}$  and  $\sigma_{zk}$  are the standard deviations of a Gaussian distribution; and  $z_g$  is the ground elevation. Brief description of RAPTAD model was reported in detail by Yamada (Yamada, Kao and Bunker, 1989; Yamada, 2004).

### 3. Material and Method

#### 3.1. Study Site

The study site locates in Pokhara Valley which is in Gandaki Province, the Western Region of Nepal. The altitude varies from 827 meters in the southern part to 1,740 meters in the north. The Annapurna Range, with three of the ten highest mountains in the world i.e. Dhaulagiri, Annapurna I and Manaslu, are within 24 – 56 km of the valley. The valley is approximately divided into four to six parts by the rivers Seti, Bijayapur, Bagadi, Phusre and Hemja. The Seti Gandaki flowing through the city from north to south divides the city roughly in two halves. The floor of the valley is plain, resembles Terai due to its gravel-like surface, and has slanted orientation from northwest to southeast. The city is surrounded by the hills overlooking the entire valley. Out of the total area, approximately 1% of the area is covered by water. The rest of the area is covered with agricultural land, forest and built-up areas.

Millions of domestic and international tourists visit Pokhara and its vicinity every year. Shining Himalayas, pristine lakes, caves, unique culture, pleasant environment, etc., are the major beauty of Pokhara. Pokhara Regional International Airport (PRIA) is a newly constructed airport in Pokhara. It is 3 km east from the existing domestic airport, at Chinnedanda. PRIA has one runway measuring 2,500 m length and 45 m width. The airport has concrete runway, parking bays will be able to handle up to five narrow-body aircraft. Two terminals, one

domestic and one international, will be able to handle one million passengers annually. Figure 2 shows the location of PRIA in Pokhara Valley. The study domain in this study covers the whole valley area and its surrounding area which may be affected by the pollution generated in the valley area mostly from PRIA site and its periphery. Meteorological data required for setting the initial and boundary condition of the numerical simulation study are utilized from the secondary source data of nearby station as well as from the published articles.

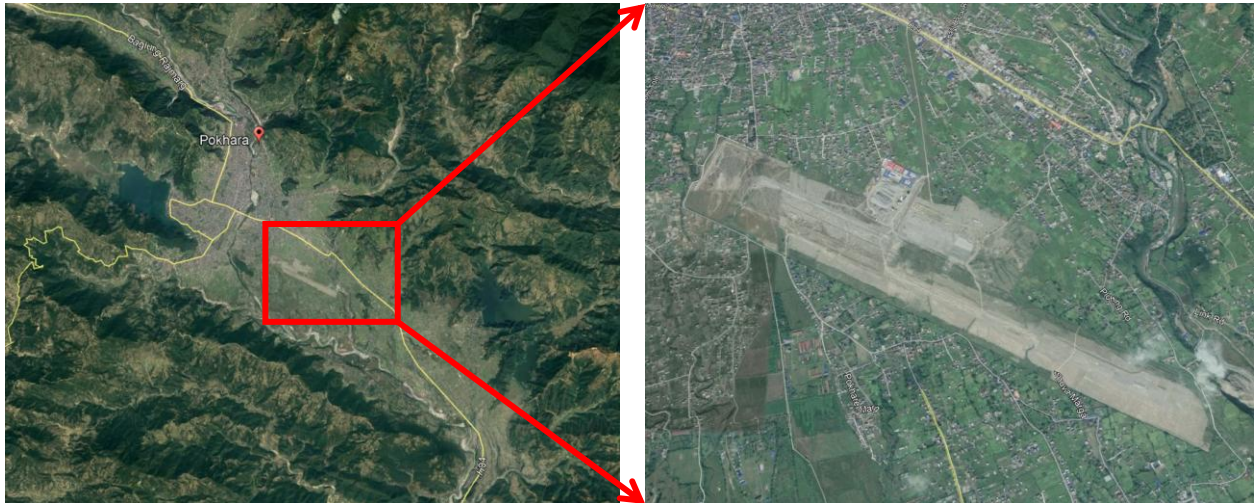


**Figure 2.** Study site covering the downtown area of Pokhara valley and its surrounding: right hand side picture shows the core firm land converted in to the buildup area.

### 3.2 Meteorological Data

Local meteorology especially, temperature, wind speed and direction play vital role for the generation, transport and dispersion of air pollution from the source to the surrounding location. Initial and boundary conditions in the modeling were set based on the available meteorology data. The meteorological data, such as wind speed, wind direction, rainfall data were retrieved from Department of Hydrology and Meteorology Pokhara. The data recorded at the station 866 which is located at  $28^{\circ}12'20.1''N$   $83^{\circ}58'24.8''E$  (6X4F+6CM) at the elevation of 827m has been referred in this study.

### 3.3 Air Flow and Air Dispersion Modelling

The structure and circulation pattern of the breeze varies in different geographic location, although many factors such as solar radiation, landuse pattern (i.e. surface albedo, roughness, soil moisture, anthropogenic heat, etc.), inversion height, potential temperature, external wind force, etc. affect its structure and pattern. The modeling domain for this study area is designed as in Fig. 3 where the sizes of outer, interim, and inner domains are  $42\text{ km} \times 32\text{ km}$ ,  $30\text{ km} \times 24\text{ km}$  and  $20\text{ km} \times 14\text{ km}$ , respectively. The resolutions of the outermost, interim and inner nested grids are 4 km, 2 km and 1 km, respectively.

The modeling period was selected in mid of April (Julian days 101 - 103) by considering dry and less rainy season when the potential temperature difference is sufficient for breeze generation. The Cloudless, non-rainy days were considered for increasing the accuracy of the input meteorological survey data. USGS30" resolution data (about 800m resolution at mid latitude) was used for extracting the geographic information and landuse data. The meteorology

data was used based on DHM 2018 data. The nudging and earth rotation options were set active. The rest of the parameters have been fixed as default values as summarized in the A2C manual.

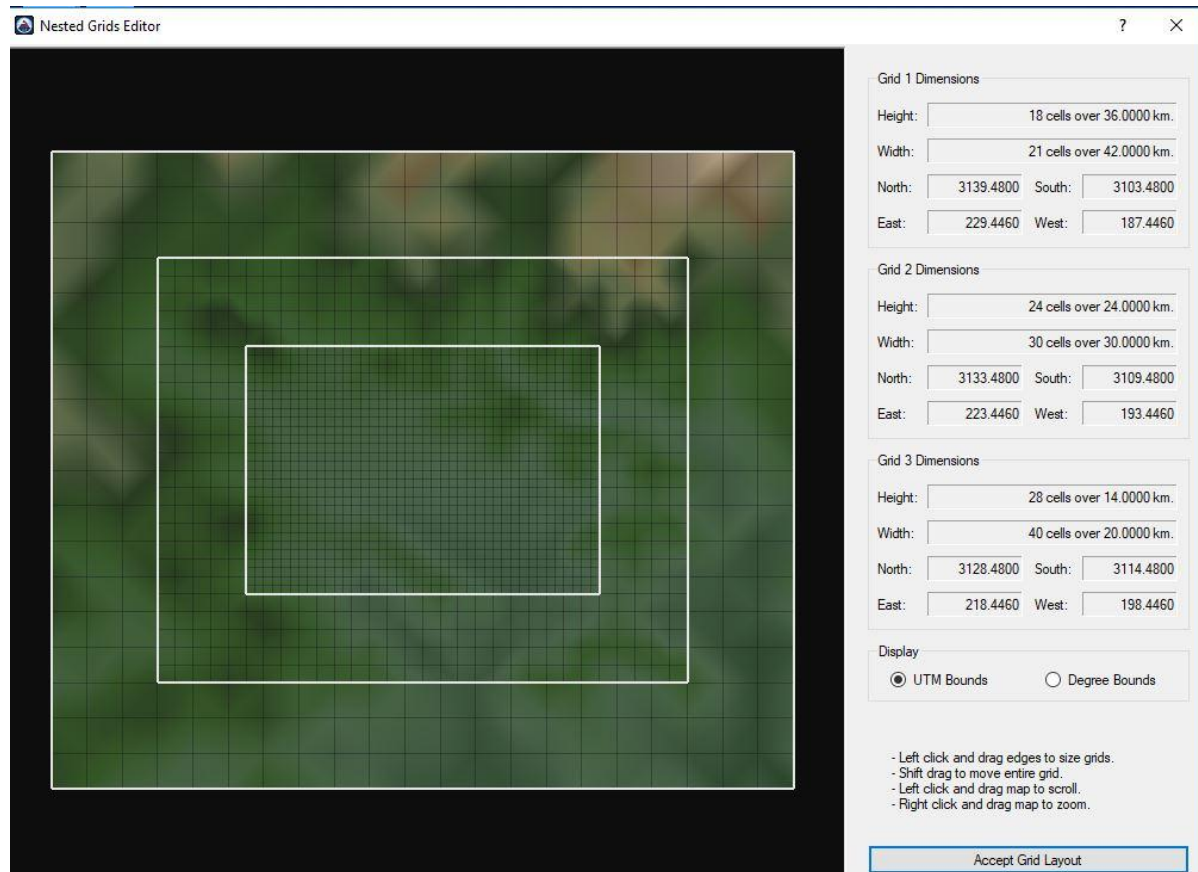


**Figure 3.** Modeling domain in different resolutions at outermost, interim and inner nested grids.

Two different techniques were applied for understanding the breeze structure and its influencing zone. In the first case, the breeze speed was sampled at different locations. In the second case, the point source Ps1 was set at the centre of the focused study site, where the puffs as emission continuously emitted from the area source with the diameter of 100 m and an altitude of 10 m. The puffs emitted from the point source were dispersed and transported by the breeze generated in the study domain. The structure of the pure breeze and its effective boundary length were estimated by analyzing wind speed, wind flow vectors and puffs dispersion patterns, respectively.

## 4. Results and Discussion

### 4.1 Meteorology of the Study Site

There are distinct four seasons in Pokhara where months from November to February are cold. Other months except midday of May – June are comfortable and warm. In general, winter months are dry and summer months are wet. More than 70% of annual rainfall has been observed during three months from June to August (Pokhrel and Ghimire, 2020). Majority of wind blows from north to south during the winter period and vice versa in the summer period. Figure 4 shows the wind speed and direction in different season of the year 2018. Most of the cases, wind blows from east and south-east direction with wind speed of 3 – 8 m/s in Pokhara. More than 10 m/s wind speed was frequently observed during the pre-monsoon period when

wind blows frequently from north-east and south-east direction. The high wind speed blows the fugitive dust from the surface and concentration of windblown dust can be observed in the pre-monsoon season than another season.

**Table 1.** Input parameters for the pure breeze modeling.

Parameters	Values	Remarks
Modeling domain	Nested grids = 3	$42 \times 36$ , $30 \times 24$ , $20 \times 14$ km <sup>2</sup>
Modeling period	Day = 101 - 103	Julian day
Wind speed (m/s)	0	No external wind
Wind direction	NA	
Ref. Pressure (mb)	1000	Ref. meteorological data
Potential temperature (°C)	23	Ref. meteorological data
Water temperature	25	
Height (m)	1000	As manual
Options	On	(nudging, earth rotation)

## 4.2 Air Flow Mechanism

A2C flow generates the meteorological information in the PBL based on the given initial and boundary condition data. Generally, the temperature of the earth surface varies with the variation of sun energy. The temperature differs significantly place to place due to the different landuse pattern and different specific heat capacities of landuse objects even though Sun energy is constant (Weil, 1988). In case of study area, most of the surface is covered by land and it is surrounded by green mountains followed by Himalayan in few kilometers far. After sunset, higher elevated mountain region releases heat faster than valley area, subsequently the mountain surface temperature becomes lower than the valley surface in late evening to early morning before sunrise. Consequently, the pressure above the valley surface becomes lower than pressure above the land surface which causes the dynamic air flow from mountain to the valley (mountain breeze) as in Fig. 5 (a, b and c). Mountain breeze gained its maximum speed just before sunrise around 6AM and then it reduces with the reduction on temperature difference between the surrounding mountain and the valley.

After sunrise, the high elevated land (mountain) surface heats faster than low elevated land (valley surface) as sun energy penetrates mountain surface before the valley surface. Correspondingly, the potential temperature difference between the mountain and the valley surface goes down, which results the collapse of the mountain breeze and reaches to transition stage around 9AM to 10AM. Figure 5 (d) shows the wind vectors just before the transition of mountain breeze to the valley breeze when very mild breeze can be observed. When the temperature of the mountain surface reaches considerably higher than the valley surface, the air above the mountain area rises up. Consequently, pressure above the mountain surface

becomes lower than the pressure above the valley surface where the air flows from higher pressure side to lower pressure, i.e. valley breeze as in Fig. 5 (e), (f). The mountain surface temperature diminishes faster than the valley surface temperature with the declination of sun radiation energy and hence the valley breeze continuously diminishes and reaches to the transition period again around 8PM to 10PM. The locally generated breeze and its boundary play vital role for the transport and diffusion of air pollution at that boundary. Moreover, the concentration of air pollution in certain locality vary with the varying the boundary layer (Fan et al.; Jeong, Lee and Lee, 2008; Jung, Pokhrel and Lee, 2009). A study shows that the katabatic winds had varied effects on pollution in different city regions, influenced by atmospheric conditions. Moreover, the meteorological factor such as temperature lapse rate, topography and surface coverage limit the air pollution dispersion (Shang et al., 2023).

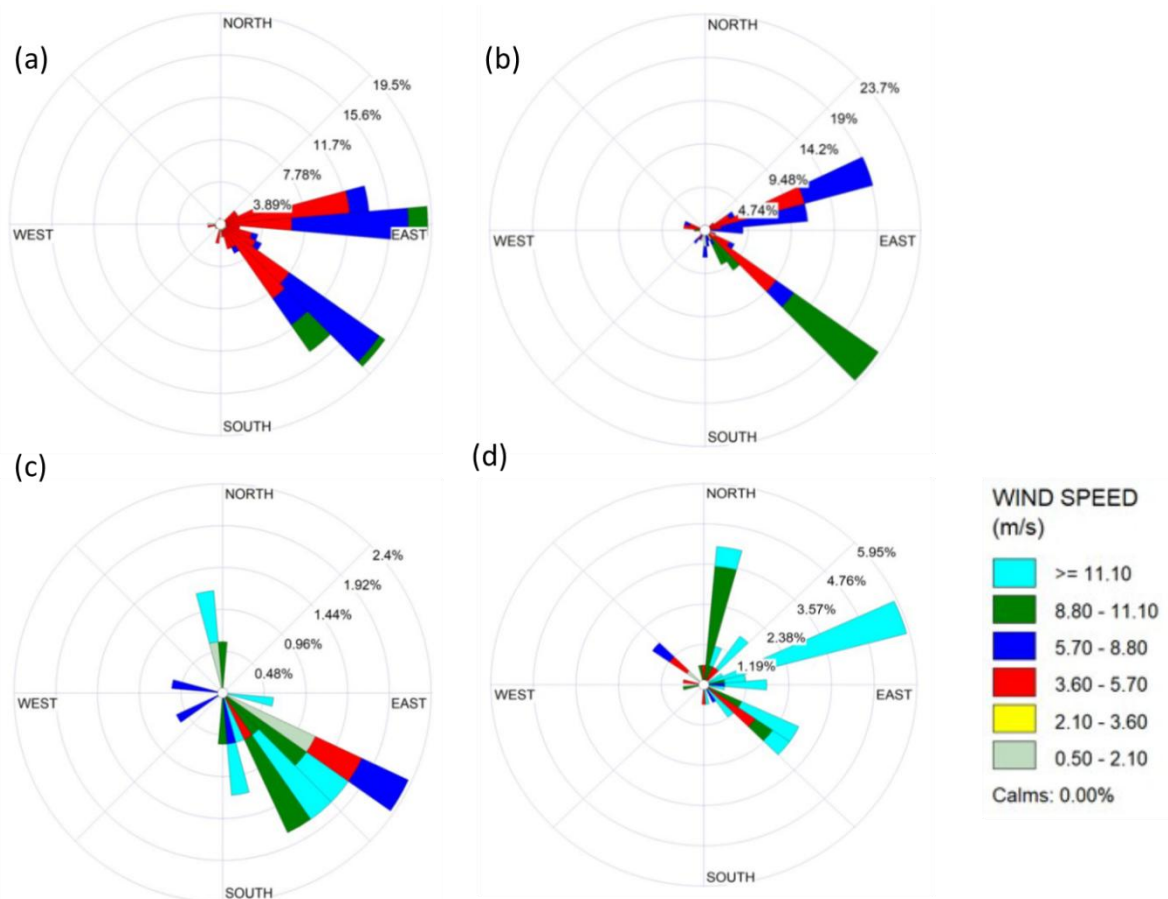
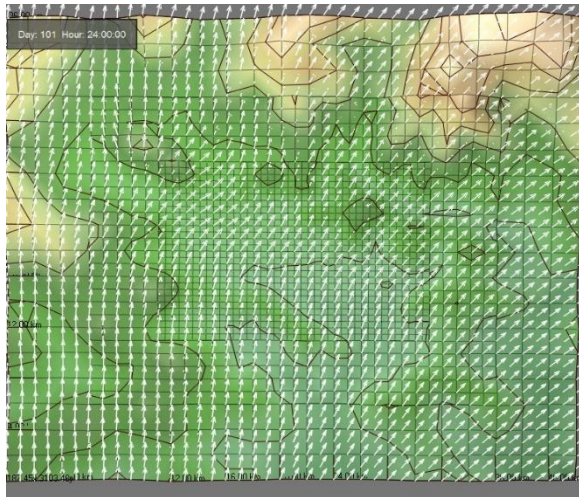
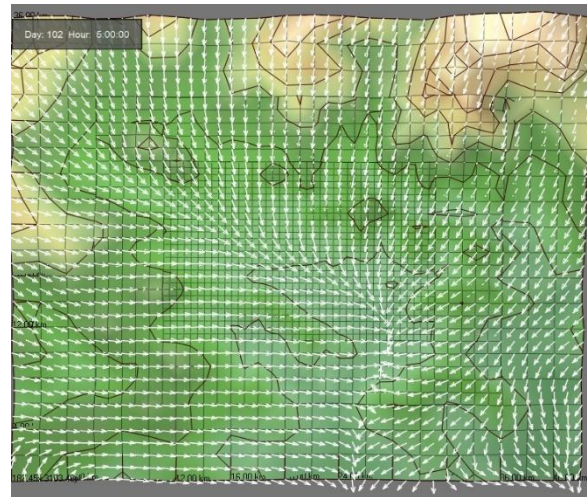


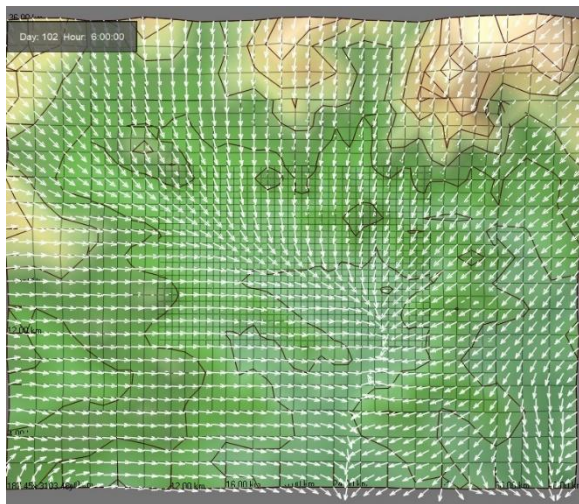
**Figure 4.** Windrose shows the wind profile during (a) Monsoon period, (b) Post-monsoon period, (c) Winter period and (d) Pre-monsoon period.



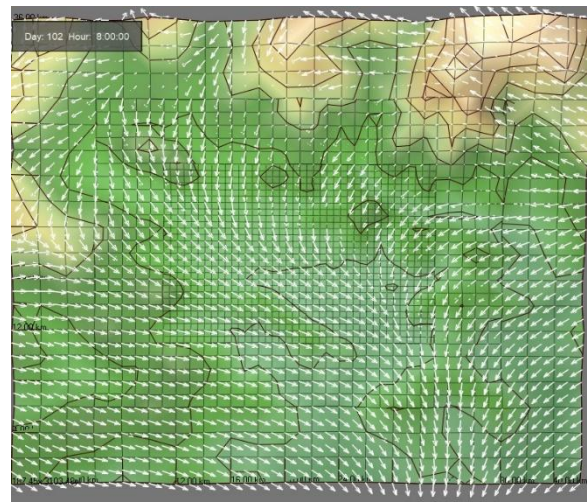
(a) Time 00:00



(b) Time 01:00



(c) Time 06:00



(d) Time 08:00



(e) Time 12:00

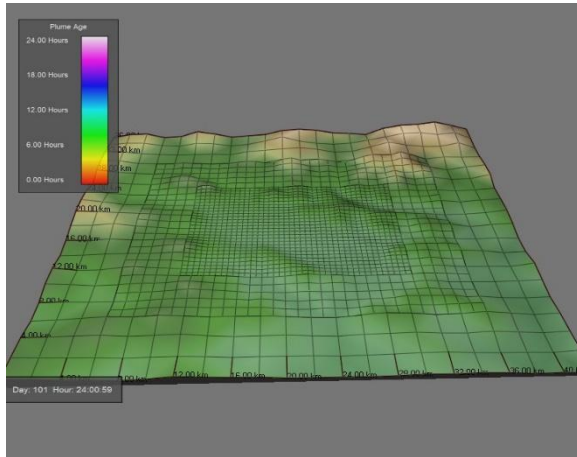


(f) Time 18:00

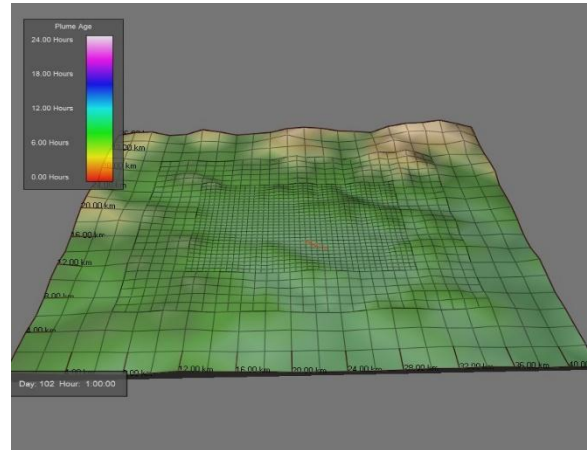
**Figure 5.** Diurnal changes of wind flow profile in the study area

### 4.3 Air Dispersion Mechanism

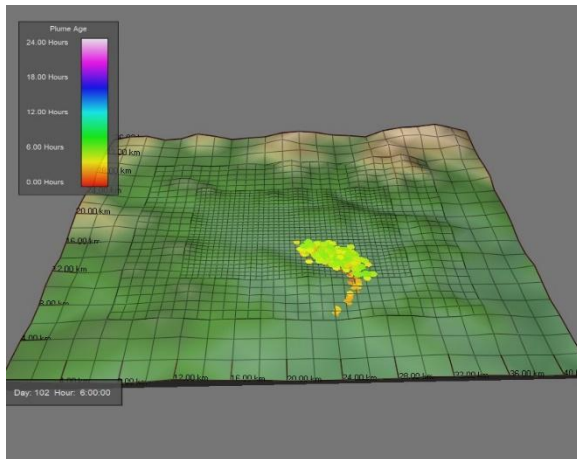
Transportation and dispersion of puffs from the sources depend on the local meteorological condition. Mountain breeze generates during late night to early morning when puffs transport and disperse to the valley side. Mountain breeze diminishes and changes to valley breeze after 10AM when the puffs near the source start to disperse towards mountain side and disperse above the mountain region as in Fig. (6).



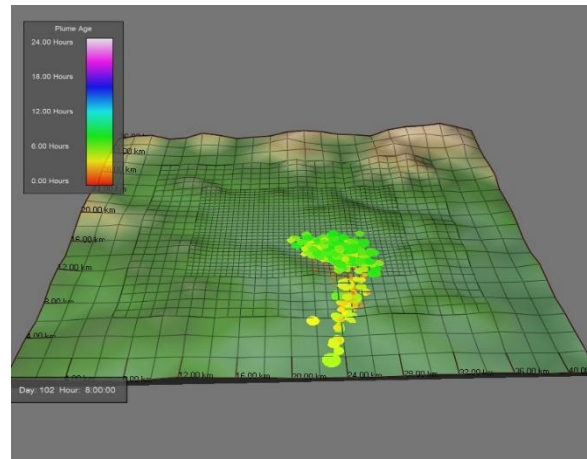
(a) Time 00:00



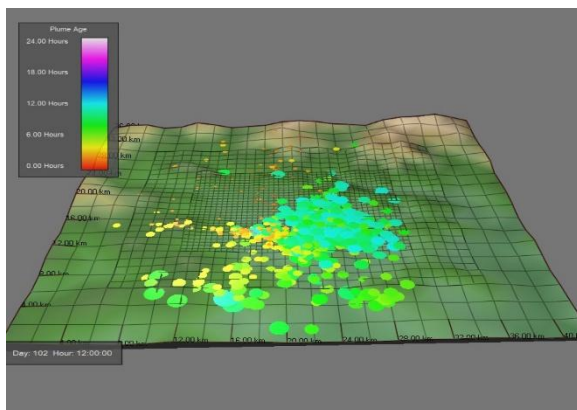
(b) Time 01:00



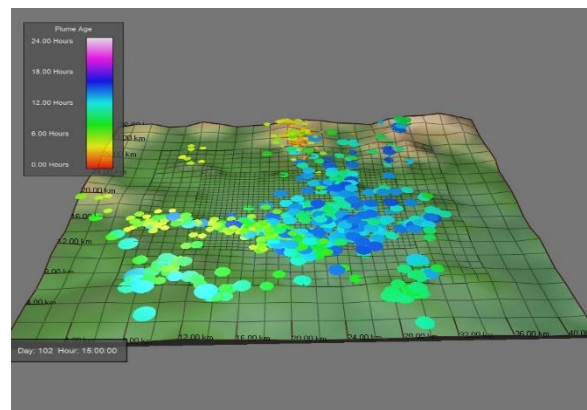
(c) Time 6:00



(d) Time 8:00



(e) Time 12:00



(f) Time 15:00

**Figure 6.** Puff dispersion from the source by locally generated breeze in the study domain.

Pokhara Regional International Airport (PRIA) has been in constructed and operation at the central area of Pokhara Valley. The puffs source in this study as in Fig. 6. (a) is located at the same location of PRIA site. The puffs in the modeling domain represent the pollutants generated from the construction site (PRIA). Figure 6 (b – f) shows the puff dispersion mechanism from source to the surrounding area at different time period. Puffs from the source transports towards south from late-night to the early-morning and it disperses around the high-altitude mountain region in the daytime. It shows that the pollutions generated from the construction site disperse in the mountain region by the locally generated wind. Similar study was conducted in the Sichuan Basin (SCB), China to identifying the impact of mountain valley breeze on ozone pollution. The mountain valley driven near-surface O<sub>3</sub> concentrations increased by 8.8%, with 12.7% and 50.0% deterioration in the O<sub>3</sub> light and moderate exceedance rates, respectively, on the western SCB edge (Zhang et al., 2024). Urban air pollutions generated from different sources such as construction site, industries, commercial sector, vehicular / aviation emission disperse inside the valley and its surrounding mountainous area. It may affect the air quality of the pristine mountain region. Therefore, policy should be developed for planned urbanization by considering urban air quality, bio-ecosystem and climate resilient society.

## 5. Conclusion

Pokhara has been recognized as one of the beautiful valleys because of its pristine nature and cool and clean environment. The valley has been changed rapidly in terms of its landuse as well as air quality. Local meteorology directly affected the urban comfort as well as air quality of the valley due to its driving effect on air pollution dispersion. Majority of breeze flows from north to south and vice-versa in Pokhara whereas the external wind dominates during the pre-monsoon period. A study was conducted to identify the air pollution dispersion mechanism in the valley using Lagrangian Approach. The simulation results for the study domain revealed that the air flows from the mountain region to the valley from the mid night to the early morning around 8 AM. As the mountain region get heated, the flow velocity decreases and reaches to the transition state around 09:00 AM – 10:00 AM. Then flow direction changes towards the Mountain region after 11 AM and wind speed is maximum around 2 PM to 3 PM. It is continuous till mid-night around 9 PM to 10 PM and again reaches to the transition period.

Urban air pollution generated in the valley area accumulated in the valley region in the mid-night to the early morning due to the effect of mountain breeze and it disperses around the upper air mostly above the mountain region. Mostly, the pollution generated nearby the mountain region disperses above the mountain region in the daytime. The pollution generated near the mountain region has significantly less impact to urban area where as the pollution generated from the urban area affects the air quality in the mountain region. Locally generated wind speed and its boundary plays the vital role for maintaining in the valley. It is concluded that the pollution generated from the different sources disperses around the valley and reached up to the mountain region which may degrade the quality of scenic vista.

## Acknowledgements

This research is partially supported by Pokhara University Research Center funded research grant number 01/074/75 (FRG AC). I would to thank all the supporting hands for completing this research.

## References

- Fan, S., Wang, B., Tesche, M., Engelmann, R., Althausen, A., Liu, J., Zhu, W., Fan, Q., Li, M., Ta, N., Song, L., Leong, K., 2008. Meteorological condition and structures of atmospheric boundary layer in October 2004 over Pearl River Delta area. *Atmospheric Environment*, 42, 6147-6186.
- Jacob, D. J., 1999. *Introduction to atmospheric chemistry*. Princeton University Press.
- Jeong, J., Lee, I.H., Lee, H., 2008. Estimation of the effective region of Sea/Land breeze in west coast using numerical modeling. *Journal of Korean Society for Atmospheric Environment*, 24, 2, 259-270.
- Jung, C.H, Pokhrel, R., Lee, H.K., 2009. The impact of power plants on the environment and region – Focus on Incheon area according to the 3rd electric support action plan. *Journal of Environmental Impact Assessment Korea*, 18, 4, 195-208.
- Laña, I., Ser, J. D., Padró, A, Vélez, M., Casanova-Mateo, C., 2016. The role of local urban traffic and meteorological conditions in air pollution: A data-based case study in Madrid, Spain. *Atmospheric Environment*, 145, Pages 424-438. <https://doi.org/10.1016/j.atmosenv.2016.09.052>.
- Pokhrel, R., Lee, H., 2011. Estimation of the effective zone of sea/land breeze in a coastal area. *Atmospheric Pollution Research*, 2, 106-115.
- Pokhrel, R., Ghimire, S. (2020) *Numerical Simulation on Air Pollution Emission from the Construction Site and Its Dispersion in the Pokhara Valley*. PURC, Pokhara University.
- Shang, J., Zhong, H-Y., Zhang, H-L., Li, B., Wang, X-X., Zhao, F-Y., Li, Y., 2023. Diode effects on street canyon ventilation in valley city: Temperature inversion and calm geostrophic wind. *Building and Environment*. 244, 10839.
- Wond, N H., Chen, Y., 2009. *Tropical Urban Heat Island: Climate, Buildings and Greenery*. Taylor and Francis.
- Weil, J. C., 1988a. *Dispersion in the convective boundary layer: Lectures on Air Pollution Modeling*. Venkatram, A. and Wyngaard, J. C. American Meteorological Society, 167-227.
- Yamada, T., 1981. A numerical simulation of nocturnal drainage flow. *Journal of The Meteorological Society of Japan*, 59, 108-122.
- Yamada, T., Kao, J.C.Y., Bunker, S., 1989. Airflow and air quality simulations over the western mountainous region with a four-dimensional data assimilation technique. *Atmospheric Environment* 23, 539-554.
- Yamada, T., 1999. A numerical simulation of urbanization on the local climate. *Journal of Wind Engineering and Industrial Aerodynamics*, 81, 1-19.
- Yamada, T., 2004. Merging CFD and atmospheric modeling capabilities to simulate airflows and dispersion in urban areas. *Journal of Computational Fluid Dynamics (CFD J.)* 13(2):47, 329-341.
- Zhang, Y., Zhao, T., Sun, X., Bai, Y., Shu, Z., Fu, W., Lu, Z., Wang, X., 2024. Ozone pollution aggravated by mountain-valley breeze over the western Sichuan Basin, Southwest China. *Chemosphere*, 361, 142445. <https://doi.org/10.1016/j.chemosphere.2024.142445>